



FRACTIONAL-ORDER DENGUE VIRUS MODEL WITH VECTOR AND NON-VECTOR TRANSMISSION: BIFURCATION ANALYSIS AND MEMORY EFFECTS

*¹Ahman, Q. Ojoma, ¹Joseph, S. Onuche, ²John, S. Onuche, ¹Adaji, Isacc and ³Ezaegu, V. Ikechukwu

¹Department of Mathematics/Statistics, Confluence University of Science and Technology, Osara. Kogi State, Nigeria.

²Department of Mathematics, University of Nigeria, Nsukka, Nigeria

³Department of Mathematics, Ebonyi State University, Abakiliki Nigeria

*Corresponding authors' email: ahmanqo@custech.edu.ng

ABSTRACT

Dengue fever, a major mosquito-borne disease, poses significant global health challenges, particularly in tropical and subtropical regions. Traditional epidemiological models often fail to capture the memory-dependent dynamics and complexities of disease transmission, limiting their effectiveness in informing public health strategies. This study introduces a novel fractional-order dengue transmission model using the Caputo fractional derivative to incorporate memory effects. The model considers both vector and non-vector transmission pathways, along with mosquito-to-mosquito transmission. The basic reproduction number (R_0) was derived using the next-generation matrix method. Stability analyses were performed to explore the conditions under which backward bifurcation occurs, with a particular focus on the influence of mosquito-to-mosquito transmission dynamics. Stability analysis revealed that backward bifurcation arises when the reproduction number associated with mosquito-to-mosquito transmission exceeds one, highlighting its critical role in dengue dynamics. Numerical simulations demonstrated that fractional-order models effectively delay epidemic peaks and extend the transition period of exposed populations, providing extended windows for timely interventions. Sensitivity analysis identified mosquito-to-human and mosquito-to-mosquito transmission rates as key drivers of R_0 emphasizing the need for targeted control measures, including vector control and vaccination campaigns. This study demonstrates that fractional-order models are superior to traditional integer-order models in capturing the complex dynamics of dengue transmission. By integrating memory effects and analyzing critical transmission pathways, the model offers a more realistic framework for understanding dengue spread. These findings provide valuable insights for optimizing public health interventions, emphasizing the transformative potential of fractional-order models in sustainable dengue control and future research.

Keywords: Dengue transmission, Fractional order modelling, Backward Bifurcation, Mosquito-to-mosquito transmission, Human-to-human transmission

INTRODUCTION

Dengue virus (DENV) is one of the most prevalent vector-borne diseases, affecting millions globally each year, with outbreaks increasingly observed in tropical and subtropical regions. The complex nature of its transmission dynamics, involving human hosts and *Aedes Aegypti* mosquitoes, necessitates advanced mathematical modeling approaches to understand and predict its spread. Traditional epidemiological models, such as those based on the SIR framework, have been instrumental in understanding dengue virus dynamics. However, these models often rely on integer-order derivatives that may not fully capture the memory-dependent and complex interactions inherent in disease transmission. To address these limitations, fractional-order calculus has emerged as a robust mathematical tool that provides a more realistic representation of biological systems, incorporating memory effects and non-local interactions (Alshehry et al. 2024; Nasir et al. 2024)

Several researchers have emphasized the importance of fractional-order modeling in understanding the intricacies of dengue virus transmission. (Alshehry et al. 2024) employed the Caputo–Fabrizio fractional derivative to refine dengue transmission models, showcasing its ability to address non-singular kernel dynamics and improve computational efficiency. Meena and Purohit (2024) contributed by exploring mathematical analysis using fractional operators, further validating their effectiveness in studying dengue's nonlinear dynamics.

The Caputo fractional derivative, in particular, has gained traction for its ability to generalize classical models while maintaining mathematical rigor and computational efficiency (Olayiwola & Yunus. 2024; Usman et al. 2024). Studies incorporating this derivative have explored various interventions, such as quarantine measures, vaccination campaigns, and vector control strategies, emphasizing the real-world applicability of fractional models (Pandey & Phaijoo, 2024; Meetei et al. 2024). Moreover, advanced numerical methods and optimal control approaches have been developed to enhance the analysis of fractional-order models (Vijayalakshmi et al. 2024; Adel et al. 2024).

Regional studies have also contributed to understanding dengue's transmission dynamics in specific contexts. Pandey and Phaijoo (2024) used a fractional Caputo model with optimal control strategies to analyze dengue in Nepal, while Asaduzzaman et al. (2024) tailored a fractional-order ASIR model for Bangladesh, underscoring the value of context-specific approaches (Pandey & Phaijoo, 2024; Asaduzzaman et al. 2024). These studies demonstrate how regional factors, such as vaccination rates, public health infrastructure, and mosquito control efforts, can influence epidemic outcomes. Several works have delved deeper into the biological underpinnings of dengue transmission. Olayiwola and Yunus (2024) examined within-host dengue virus dynamics, integrating adaptive immunity into their fractional-order models. Xu et al. (2024) provided a quantitative analysis of host-virus interactions, emphasizing the importance of

including biological and immunological factors in modeling efforts.

A review by Nisar et al. (2024) consolidated the applications of fractional-order epidemic models, highlighting their evolution and future potential in tackling complex life sciences problems. Additionally, Sk et al. (2024) examined the global stability and optimal control of fractional-order transmission and recovery processes, stressing the influence of fractional parameters on DENV disease progression. Studies by Islam et al. (2024) and Naaly et al. (2024) reinforced these findings by integrating public health strategies, such as mass awareness campaigns and vector control measures, into fractional models.

Other innovative approaches include those by Olayiwola and Alaje (2024), who investigated antigenic immunity and its impact on dengue dynamics, and Meetei et al. (2024), who utilized compartmental fractional-order models to refine our understanding of dengue transmission. Further, studies by Vellappandi et al. (2024) and Kumar et al. (2024) explored optimal control problems and transmission dynamics using Caputo fractional derivatives, highlighting their ability to model real-world complexities effectively.

Finally, advancements in computational methods, such as those by El-shenawy et al. (2024) and Adel et al. (2024), have improved the simulation and analysis of fractional-order systems, making them more accessible for public health applications. Shanmugam and Byeon (2024) extended these insights by reviewing analytical methods across multiple diseases, demonstrating the broader applicability of fractional models in epidemiology.

The present study advances this extensive body of work by developing a novel fractional-order dengue transmission model that incorporates both vector and non-vector transmission pathways. Unlike previous studies, this model integrates detailed epidemiological transitions, such as susceptibility, exposure, infection, vaccination, and recovery, within a fractional-order framework. Using the Caputo fractional derivative, the model captures memory effects and delayed interactions to better reflect the real-world complexity of dengue virus epidemics. The next-generation matrix methodology is employed to derive the basic reproduction number, a critical threshold parameter that determines the potential for disease outbreaks. Stability analysis is performed to assess the equilibrium states, providing insights into the long-term behavior of the system. Numerical simulations were conducted to explore the dynamics of the disease under varying conditions, offering practical strategies for controlling the spread of dengue and enhancing public health interventions.

MATERIALS AND METHODS

To address the limitations of traditional DENV transmission models and provide a more comprehensive understanding of DENV dynamics, this study presents a fractional-order mathematical model for dengue virus transmission, incorporating both vector and non-vector pathways, as well as mosquito-to-mosquito transmission dynamics. The model utilizes the Caputo fractional derivative to account for memory effects inherent in biological systems. Key epidemiological compartments are defined, including susceptible, exposed, infected, vaccinated, and recovered populations.

DENV Integer -Order Model formulation

In formulating the Dengue fever Integer order model, we assume that; (i) Dengue is transmitted between humans and mosquitoes, human-to-human and mosquito-to-mosquito

transmission. (ii) Humans are divided into susceptible, exposed, infectious, and recovered compartments and Mosquitoes are divided into susceptible, exposed, and infectious compartments. (iii) Humans and mosquitoes mix homogeneously. (iv) Both humans and mosquitoes experience a non-infectious incubation period after acquiring the virus. (v) Recovered humans are assumed to have temporal immunity to reinfection. (vi) The mosquito biting rate is constant. (vii) Both humans and mosquitoes experience disease-related mortality rate.

We divided the Human population into five (5) compartments; Dengue fever susceptible compartment H_S , Dengue fever imperfect vaccinated compartment H_V , Dengue fever exposed compartment H_E , Dengue virus infectious compartment H_I and Dengue fever recovered compartment H_R . We equally divided the Mosquito population into three (3) compartments; Dengue fever susceptible mosquitoes' compartment M_S , Dengue fever exposed mosquitos' compartment M_E and Dengue fever infectious mosquitos' compartment M_I . The total human population is represented by T_h while the total mosquito population is represented by T_m and Total population given as T_{im} .

Dengue fever Susceptible Compartment H_S , is recruited at the rate of Λ_H . The compartment reduces by natural death rate μ_h and also by the proportion of humans becoming infected after having contacts with either Dengue fever infected human or Dengue fever infected mosquitoes at rate of β_h (either Dengue fever infected human at the rate ρ_1 or Dengue fever infected mosquito at the rate $\rho_2\omega$ with ω as the mosquito biting rate) and the rate of vaccination ε . This compartment also grows by the rate that the recovered loses immunity ϕ_h and by the rate at which the vaccine wanes so that the vaccinated becomes susceptible again at the rate σ .

We therefore formulated the dynamics of Dengue fever susceptible compartment as;

$$\frac{dH_S}{dt} = \Lambda_H + \phi_h H_R + \varepsilon H_V - (\mu_h + \sigma + \beta_h) H_S \quad (1)$$

Imperfect Vaccinated Human Compartment H_V grows due to vaccination

Rate ε and the compartment reduces due to vaccine waning rate σ and natural death at rate μ_h . The dynamics of Dengue fever vaccinated compartment is modeled as follows;

$$\frac{dH_V}{dt} = \sigma H_S - (\mu_h + \varepsilon) H_V \quad (2)$$

Dengue fever Exposed Human Compartment H_E increases as a result of the proportion

Of individuals that are infected newly at the rate of β_h . This class reduces by the rate at which the exposed becomes fully infectious at rate θ_h and by natural death rate μ_h . This Population is formulated as follows;

$$\frac{dH_E}{dt} = \beta_h H_S - (\mu_h + \theta_h) H_E \quad (3)$$

Dengue fever Infectious Human Compartment H_I grows due to the progression of

The exposed to the infected class at rate θ_h . The population reduces by natural death rate μ_h , death due to dengue virus disease at rate δ_h and due to recovery rate τ_h . The dynamics of this compartment is formulated as;

$$\frac{dH_I}{dt} = \theta_h H_E - (\mu_h + \delta_h + \tau_h) H_I \quad (4)$$

Dengue fever Recovered Human Compartment H_R grows due to recovery rate τ_h . The compartment reduces due to natural death at rate μ_h and those that recovered losing immunity at the rate ϕ_h . The dynamics of this class is formulated as;

$$\frac{dH_R}{dt} = \tau_h H_I - (\mu_h + \phi_h) H_R \quad (5)$$

Dengue fever Susceptible Mosquito Compartment M_S is recruited at rate Λ_M . The compartment reduces by the rate at which the susceptible mosquitoes becomes infected after

having contact with infected humans or infected mosquitoes at rate β_m (either Dengue fever infected human at the rate $\eta_1\omega$ or Dengue fever infected mosquito at the rate η_2 with ω as the mosquito biting rate) and by natural death of mosquitoes at rate μ_m . The dynamics of this compartment is formulated as;

$$\frac{dM_S}{dt} = \Lambda_M - (\mu_m + \beta_m)M_S \tag{6}$$

Dengue fever Exposed Mosquito Compartment M_E grows at the rate by which the

Newly infected susceptible mosquitoes progress to the exposed class at the rate β_m , the class reduces due to the rate by which the exposed mosquitoes become fully infected at the rate θ_m

And by mosquitoes' natural death rate μ_m . The dynamics of this class is formulated as follows;

$$\frac{dM_E}{dt} = \beta_m M_S - (\mu_m + \theta_m)M_E \tag{7}$$

Dengue fever infectious Mosquito Compartment M_I grows due to the progression of the exposed that becomes fully infectious at rate θ_m . This compartment reduces due to natural mosquitoes' death at the rate μ_m and finally death due to disease at the rates δ_m . The equation that corresponds to this compartment is presented as;

$$\frac{dM_I}{dt} = \theta_m M_E - (\mu_m + \delta_m)M_I \tag{8}$$

The Dengue model schematic diagram is shown in Figure 1

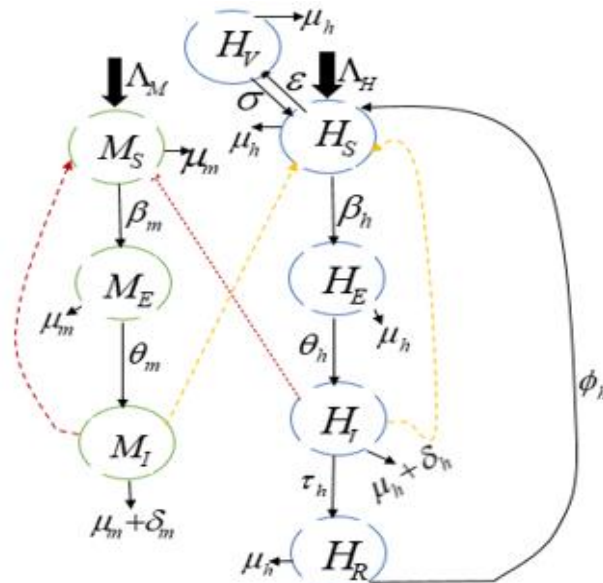


Figure 1: Dengue Model Schematic Diagram

The mathematical model equation that corresponds to our description above is given by;

$$\left. \begin{aligned} (a) \quad & \frac{dH_S}{dt} = \Lambda_H + \phi_h H_R + \sigma H_V - (\mu_h + \varepsilon + \beta_h)H_S \\ (b) \quad & \frac{dH_V}{dt} = \varepsilon H_S - (\mu_h + \sigma)H_V \\ (c) \quad & \frac{dH_E}{dt} = \beta_h H_S - (\mu_h + \theta_h)H_E \\ (d) \quad & \frac{dH_I}{dt} = \theta_h H_E - (\mu_h + \delta_h + \tau_h)H_I \\ (e) \quad & \frac{dH_R}{dt} = \tau_h H_I - (\mu_h + \phi_h)H_R \\ (f) \quad & \frac{dM_S}{dt} = \Lambda_M - (\mu_m + \beta_m)M_S \\ (g) \quad & \frac{dM_E}{dt} = \beta_m M_S - (\mu_m + \theta_m)M_E \\ (h) \quad & \frac{dM_I}{dt} = \theta_m M_E - (\mu_m + \delta_m)M_I \end{aligned} \right\} \tag{9}$$

And the dengue rate of infectivity for both populations β_h and β_m defined as follows;

$$\beta_h = \frac{\rho_1 H_I + \rho_2 \omega M_I}{T_{hm}} \text{ and } \beta_m = \frac{\eta_1 \omega H_I + \eta_2 M_I}{T_{hm}} \tag{10}$$

The dengue virus model variables and parameter descriptions are presented in Table 1 and Table 2 respectively.

Dengue Virus Model Variables and Parameter Descriptions, Values and Source

Table 1: DENV Model Variables Description

Variables	Description	Values	Source
H_S	DENV Susceptible human Class	406,250	Mohammed et al. (2022)
H_V	DENV Vaccinated human Class	20000	Mohammed et al. (2022)
H_E	DENV Exposed human Class	369,150	Mohammed et al. (2022)
H_I	DENV Infectious human Class	156,170	Mohammed et al. (2022)
H_R	DENV Recovered human Class	20,000	Mohammed et al. (2022)
M_S	DENV Susceptible Mosquitoes Class	40,200	Mohammed et al. (2022)
M_E	DENV Exposed Mosquitoes Class	32,000	Mohammed et al. (2022)
M_I	DENV Infectious Mosquitoes Class	21,200	Mohammed et al. (2022)

Table 2: DENV Model Parameters Description

Parameters	Description	Value	Source
Λ_H	Human recruitment rate	0.0000406	Mohammed et al. (2022)
Λ_M	Mosquito recruitment rate	0.0005789	Naaly et al. (2024)
ε	Human Imperfect vaccination rate	0.8	Mohammed et al. (2022)
σ	Vaccine waning rate	0.25	Mohammed et al. (2022)
θ_h	Exposed to Infectious human progression rate	0.1667	Naaly et al. (2024)
θ_m	Exposed to Infectious Mosquito progression rate	0.1428	Naaly et al. (2024)
τ_h	Infectious to Recovered Human progression rate	0.14286	Naaly et al. (2024)
ϕ_h	Recovered to Susceptible Human progression rate	0.011	Naaly et al. (2024)
μ_h	Human natural death rate	0.0000457	Naaly et al. (2024)
μ_m	Mosquito natural death rate	0.03	Naaly et al. (2024)
δ_h	Human DENV disease death rate	0.33	Mohammed et al. (2022)
δ_m	Mosquito DENV disease death rate	0.05	WHO (2022)
ω	Biting rate of Mosquitoes	0.5	Naaly et al. (2024)
ρ_1	Human -to-human transmission probability rate	0.001	Rahman et al. (2022)
ρ_2	Mosquito -to-human transmission probability rate	0.375	Naaly et al. (2024)
η_1	Human -to-mosquito transmission probability rate	0.375	Naaly et al. (2024)
η_2	Mosquito -to-mosquito transmission probability rate	0.02	Chitnis et al. (2021)

DENV Fractional -Order Model Formulation

We apply in this section some basic definitions from fractional calculus with the right and left fractional Caputo derivative as defined and applied in Atokolo et al. (2024). Herein, we extend the integer order model of Dengue fever presented in Equation (9) using Caputo fractional derivative operator. The new DENV mathematical model presented using Caputo fractional derivative operator has a higher degree of freedom as compared to the integer order model presented in Equation (9), as fractional order model output can be varied to have different responses. The fractional Dengue fever mathematical model equation is therefore presented as follows;

$$\left. \begin{aligned}
 (a) \quad & {}^c D_t^\alpha H_S = \Lambda_H + \phi_h H_R + \sigma H_V - B_1 H_S \\
 (b) \quad & {}^c D_t^\alpha H_V = \varepsilon H_S - B_2 H_V \\
 (c) \quad & {}^c D_t^\alpha H_E = \beta_h H_S - B_3 H_E \\
 (d) \quad & {}^c D_t^\alpha H_I = \theta_h H_E - B_4 H_I \\
 (e) \quad & {}^c D_t^\alpha H_R = \tau_h H_I - B_5 H_R \\
 (f) \quad & {}^c D_t^\alpha M_S = \Lambda_M - B_6 M_S \\
 (g) \quad & {}^c D_t^\alpha M_E = \beta_m M_S - B_7 M_E \\
 (h) \quad & {}^c D_t^\alpha M_I = \theta_m M_E - B_8 M_I
 \end{aligned} \right\} \quad (11)$$

Where;

$$\left. \begin{aligned}
 B_1 = (\mu_h + \varepsilon + \beta_h), B_2 = (\mu_h + \varepsilon), B_3 = (\mu_h + \theta_h), B_4 = (\mu_h + \delta_h + \tau_h), \\
 B_5 = (\mu_h + \phi_h), B_6 = (\mu_m + \beta_m), B_7 = (\mu_m + \theta_m), B_8 = (\mu_m + \delta_m)
 \end{aligned} \right\} \quad (12)$$

Subject to the initial conditions;

$$\left. \begin{aligned}
 H_S = H_{S0} > 0, H_V = H_{V0} \geq 0, H_E = H_{E0} \geq 0, H_I = H_{I0} \geq 0, H_R = H_{R0} \geq 0, \\
 M_S = M_{S0} > 0, M_E = M_{E0} \geq 0 \text{ and } M_I = M_{I0} \geq 0
 \end{aligned} \right\} \quad (13)$$

DENV Model analysis

In this section, we herein analyze the dynamic system of fractional DENV mathematical model in equation (11) as follows;

Positivity of Solutions

Herein, we show that the closed set $\Omega_{hm} = \{(H_S, H_V, H_E, H_I, H_R, M_S, M_E, M_I) \in \mathbb{R}_+^8 : 0 \leq T_{hm}\}$ provides the fractional DENV dynamic system (11) positively invariant feasible region.

Theorem 1

The solutions of the fractional DENV mathematical model system (11) are non-negative and bounded if they start in Ω_{hm} .

Proof

To mathematically prove positivity of solutions for the DENV fractional model in equation (11), we invoke the Comparison Theorem which applies because if the derivative $\frac{dx}{dt}$ is non-negative whenever $x(t) = 0$ then $x(t)$ cannot decrease below zero. Thus, we apply the comparison theorem to equation (11) to ensure that each of the model state variables $(H_S, H_V, H_E, H_I, H_R, M_S, M_E, M_I)$ remains non-negative if it starts with non-negative initial value.

For equation (11)(a);

At $H_S = 0$ the equation becomes $\frac{dH_S}{dt} = \Lambda_H + \phi_h H_R + \varepsilon H_V \geq 0$ since all variables and parameters are positive.

Thus,

$$H_S(t) \geq 0 \quad \forall t \geq 0.$$

Similarly for equations (11) (b) – (h), we obtained the following;

$$\left. \begin{aligned}
 {}^c D_t^\alpha H_S|_{H_S=0} &= \Lambda_H + \phi_h H_R + \varepsilon H_V \geq 0 \\
 {}^c D_t^\alpha H_V|_{H_V=0} &= \sigma H_S \geq 0 \\
 {}^c D_t^\alpha H_E|_{H_E=0} &= \beta_h H_S \geq 0 \\
 {}^c D_t^\alpha H_I|_{H_I=0} &= \theta_h H_E \geq 0 \\
 {}^c D_t^\alpha H_R|_{H_R=0} &= \tau_h H_I \geq 0 \\
 {}^c D_t^\alpha M_S|_{M_S=0} &= \Lambda_M \geq 0 \\
 {}^c D_t^\alpha M_E|_{M_E=0} &= \beta_m M_S \geq 0 \\
 {}^c D_t^\alpha M_I|_{M_I=0} &= \theta_m M_E \geq 0
 \end{aligned} \right\} \quad (14)$$

Since all the model parameters and variables are positive. We therefore conclude that all state variables $(H_S, H_V, H_E, H_I, H_R, M_S, M_E, M_I)$ remain non-negative for all time $t \geq 0$ provided the initial conditions are non-negative. Also, as $T_{hm} = T_h + T_m$ wherever T_{hm} is considered to be constant each of the sub-population will lie in $[0, T_{hm}]$. Thus, the sub-populations $H_S, H_V, H_E, H_I, H_R, M_S, M_E$ and M_I are also bounded. This implies that all the DENV model state variables cannot decrease below zero which ensures its positivity. Therefore, the total populations of both humans and mosquitoes remain bounded for all time t and the state variables stay within the biologically meaningful region Ω_{hm} . Thus, the region Ω_{hm} is invariant under the dynamics of the system (11), meaning that if the initial conditions lie within Ω_{hm} the solutions will remain within this region for all

future time. Thus, the DENV model is epidemiologically, mathematically and biologically feasible.

Fractional DENV Model Equilibrium Points and Basic Reproduction Number

Equilibrium points of a fractional dynamical system such as (11) represent the states where the system remains unchanged over time. In the context of DENV transmission, these points help identify conditions under which the disease either vanishes or persists within a population. We define two key equilibrium points for the fractional-order dengue model: the Fractional DENV Disease-Free Equilibrium (ξ^f) and the Fractional DENV Endemic Equilibrium (ξ^e). Thus,

At equilibrium;

$$\left. \begin{aligned} {}^c D_t^\alpha H_S &= D_t^\alpha H_V = {}^c D_t^\alpha H_E = {}^c D_t^\alpha H_I = {}^c D_t^\alpha H_R = 0 \\ {}^c D_t^\alpha M_S &= {}^c D_t^\alpha M_E = {}^c D_t^\alpha M_I = 0 \end{aligned} \right\} \quad (15)$$

Fractional DENV Disease-Free Equilibrium (ξ^f): This corresponds to the state where no DENV infection exists in the human or mosquito populations. At this equilibrium, the model assumes that the infectious compartments are empty i.e., zero. Mathematically, the Fractional DENV Disease-Free Equilibrium (ξ^f) is given by:

$$\xi^f = \{H_S^f, H_V^f, H_E^f, H_I^f, H_R^f, M_S^f, M_E^f, M_I^f\} = \left\{ \frac{A_H}{(\mu_h + \sigma)}, \frac{\sigma A_H}{(\mu_h + \varepsilon)(\mu_h + \sigma)}, 0, 0, 0, \frac{A_M}{\mu_m}, 0, 0 \right\}$$

Where each component is expressed in terms of model parameters defined in Table 2.

Fractional DENV Endemic Equilibrium (ξ^e): This equilibrium describes the state where DENV persists in the population at a steady level. At this point, the infectious compartments have non-zero values, and the disease continues to circulate within the population. Deriving this equilibrium involves solving the system of equations (11) simultaneously. Thus, the Fractional DENV Endemic Equilibrium (ξ^e) is represented as:

$$\xi^e = \{H_S^e, H_V^e, H_E^e, H_I^e, H_R^e, M_S^e, M_E^e, M_I^e\} = \left\{ \frac{A_H + \phi_h H_R^e}{B_1}, \frac{\sigma H_S^e}{B_2}, \frac{\beta_h H_S^e}{B_3}, \frac{\theta_h H_E^e}{B_4}, \frac{\tau_h H_I^e}{B_5}, \frac{A_M}{B_6}, \frac{\beta_m M_S^e}{B_7}, \frac{\theta_m M_E^e}{B_8} \right\}$$

Where each component is expressed in terms of model parameters and infection dynamics.

Seeing that the Susceptible, Vaccinated, Exposed and Recovered human populations depends on the infectious human population while the mosquito population depends on the mosquito force of infection. This implies that at the fractional DENV endemic-equilibrium point there will always be DENV in the population at all time.

These equilibrium points serve as the foundation for analyzing the stability of the system and understanding its long-term behavior in response to control interventions.

DENV Fractional Model Basic Reproduction Number (R_0)

The DENV fractional model basic reproduction number (R_0) is a critical threshold parameter that determines whether the DENV disease can invade and persist in a population. It represents the average number of secondary infections produced by one DENV infected individual in a completely susceptible population.

To compute R_0 , we use the next-generation matrix approach used in Atokolo et al. (2024). Let F and V represent the infection and transition matrices, respectively. Considering the compartments (H_E, H_I, M_E, M_I) these matrices are defined as:

$$F = \begin{bmatrix} 0 & a_1 & 0 & a_2 \\ 0 & 0 & 0 & 0 \\ 0 & a_3 & 0 & a_4 \\ 0 & 0 & 0 & 0 \end{bmatrix} \quad V = \begin{bmatrix} B_3 & 0 & 0 & 0 \\ -\theta_h & B_4 & 0 & 0 \\ 0 & 0 & B_7 & 0 \\ 0 & 0 & -\theta_m & B_8 \end{bmatrix}$$

where F represents the rate of new infections, and V represents the rate of transitions between Infectious compartments due to recovery or death. Where,

$$a_1 = \frac{\rho_1 \omega \Lambda_H}{(\mu_h + \varepsilon) T_{hm}}, a_2 = \frac{\rho_2 \omega \Lambda_H}{(\mu_h + \varepsilon) T_{hm}}, a_3 = \frac{\eta_1 \omega \Lambda_M}{\mu_m T_{hm}}, a_4 = \frac{\eta_2 \Lambda_M}{\mu_m T_{hm}}$$

and B_3, B_4, B_7, B_8 are defined in equation (12). The basic reproduction number is given by:

$$\rho(F * V^{-1})$$

where ρ denotes the spectral radius (dominant eigenvalue) of the matrix product .

Mathematically, using MATLAB software we computed the following:

$$V^{-1} = \begin{bmatrix} \frac{1}{B_3} & 0 & 0 & 0 \\ \frac{\theta_h}{B_3 B_4} & \frac{1}{B_4} & 0 & 0 \\ 0 & 0 & \frac{1}{B_7} & 0 \\ 0 & 0 & \frac{\theta_m}{B_7 B_8} & \frac{1}{B_8} \end{bmatrix}$$

$$F * V^{-1} = \begin{bmatrix} \frac{a_1 \theta_h}{B_3 B_4} & \frac{a_1}{B_4} & \frac{a_2 \theta_m}{B_7 B_8} & \frac{a_2}{B_8} \\ 0 & 0 & 0 & 0 \\ \frac{a_3 \theta_h}{B_3 B_4} & \frac{a_3}{B_4} & \frac{a_4 \theta_m}{B_7 B_8} & \frac{a_4}{B_8} \\ 0 & 0 & 0 & 0 \end{bmatrix} \quad \text{and}$$

$$eig(F * V^{-1}) = \begin{bmatrix} 0 \\ 0 \\ \frac{[\theta_h a_1 B_3 B_4 + \theta_m a_4 B_7 B_8] - \sqrt{(\theta_h a_1 B_3 B_4 - \theta_m a_4 B_7 B_8)^2 + 4 B_3 B_4 \theta_h a_3 B_7 B_8 \theta_m a_3}}{2 B_3 B_4 B_7 B_8} \\ \frac{[\theta_h a_1 B_3 B_4 + \theta_m a_4 B_7 B_8] + \sqrt{(\theta_h a_1 B_3 B_4 - \theta_m a_4 B_7 B_8)^2 + 4 B_3 B_4 \theta_h a_3 B_7 B_8 \theta_m a_3}}{2 B_3 B_4 B_7 B_8} \end{bmatrix}$$

Thus, the basic reproduction number using the next-generation matrix is computed with MATLAB and given as:

$$R_0 = \frac{1}{2} \left[\left(\frac{a_1 \theta_h}{B_3 B_4} + \frac{a_4 \theta_m}{B_7 B_8} \right) + \sqrt{\left(\frac{a_1 \theta_h}{B_3 B_4} - \frac{a_4 \theta_m}{B_7 B_8} \right)^2 + 4 \frac{a_2 \theta_h a_3 \theta_m}{B_3 B_4 B_7 B_8}} \right]$$

With,

$$R_{0_{hh}} = \frac{a_1 \theta_h}{B_3 B_4} = \frac{\rho_1 \omega \Lambda_H \theta_h}{(\mu_h + \theta_h)(\mu_h + \delta_h + \tau_h)(\mu_h + \varepsilon) T_{hm}}, R_{0_{mm}} = \frac{a_4 \theta_m}{B_7 B_8} = \frac{\eta_2 \omega \Lambda_M \theta_m}{(\mu_m + \theta_m)(\mu_m + \delta_m) \mu_m T_{hm}}, R_{0_{mh}} = \frac{a_2 \theta_h}{B_3 B_4} = \frac{\rho_2 \omega \Lambda_H \theta_h}{(\mu_h + \theta_h)(\mu_h + \delta_h + \tau_h)(\mu_h + \varepsilon) T_{hm}} \text{ and } R_{0_{hm}} = \frac{a_3 \theta_m}{B_7 B_8} = \frac{\eta_1 \omega \Lambda_M \theta_m}{(\mu_m + \theta_m)(\mu_m + \delta_m) \mu_m T_{hm}} \quad (16)$$

Therefore,

$$R_0 = \frac{1}{2} \left[(R_{0_{hh}} + R_{0_{mm}}) + \sqrt{(R_{0_{hh}} - R_{0_{mm}})^2 + 4 R_{0_{mh}} R_{0_{hm}}} \right]$$

Where;

$R_{0_{hh}}$ is the reproduction number associated with human -to-human infection

$R_{0_{mm}}$ is the reproduction number associated with mosquito -to-mosquito infection,

$R_{0_{mh}}$ is the reproduction number associated with mosquito -to-human infection, and

$R_{0_{hm}}$ is the reproduction number associated with human -to-mosquito infection,

The implication of the model reproduction number is that when $R_0 < 1$ the disease will easily die out of the population but when $R_0 > 1$ the disease will persist or invade the population.

If the DENV fractional model disease-free equilibrium is locally asymptotically stable, then the infection will eventually die out. But,

If the DENV fractional model disease-free equilibrium is unstable, then the infection can invade the population.

This provides insights into the effectiveness of control strategies such as vaccination, vector control, and reducing contact rates.

Local Stability Analysis of The Fractional DENV Disease-free-equilibrium

Theorem 1

The DENV fractional disease- free equilibrium (ξ^f) of the system (11) is locally asymptotically stable (LAS) if $R_0 < 1$ and unstable if $R_0 > 1$.

Proof

Using the Jacobian matrix method we obtained the Jacobian matrix of model equation (11) evaluated at the fractional DENV disease free equilibrium point (ξ^f) is given as;

$$J_{\xi^f} = \begin{bmatrix} -B_1 & \sigma & 0 & -a_1 & \phi_h & 0 & 0 & -a_2 \\ \varepsilon & -B_2 & 0 & 0 & 0 & 0 & 0 & 0 \\ 0 & 0 & -B_3 & a_1 & 0 & 0 & 0 & a_2 \\ 0 & 0 & \theta_h & -B_4 & 0 & 0 & 0 & 0 \\ 0 & 0 & 0 & \tau_h & -B_5 & 0 & 0 & 0 \\ 0 & 0 & 0 & -a_3 & 0 & -B_6 & 0 & -a_4 \\ 0 & 0 & 0 & a_3 & 0 & 0 & -B_7 & a_3 \\ 0 & 0 & 0 & 0 & 0 & 0 & \theta_m & -B_8 \end{bmatrix}$$

We are to show that all the eigenvalues of Jacobian matrix J_{ξ^f} represented by (E) are all negative. Using MATLAB software, we obtained the eigenvalue of J_{ξ^f} as;

$$E = \begin{bmatrix} -B_5 \\ -B_6 \\ -\frac{1}{2} \left[(B_2 + B_1) + \sqrt{(B_2 - B_1)^2 + 4\sigma\varepsilon} \right] \\ -\frac{1}{2} \left[(B_2 + B_1) - \sqrt{(B_2 - B_1)^2 + 4\sigma\varepsilon} \right] \\ Q \end{bmatrix}$$

Where,

$$Q = Q_0\lambda^4 + Q_1\lambda^3 + Q_2\lambda^2 + Q_3\lambda^1 + Q_4\lambda^0$$

Which is the characteristic equation of four eigenvalues.

Clearly, $\lambda_1 = -B_5 < 0, \lambda_2 = -B_6 < 0, \lambda_3 = -\frac{1}{2} \left[(B_2 + B_1) + \sqrt{(B_2 - B_1)^2 + 4\sigma\varepsilon} \right] < 0$ and

$$\lambda_4 = -\frac{1}{2} \left[(B_2 + B_1) - \sqrt{(B_2 - B_1)^2 + 4\sigma\varepsilon} \right] < 0$$

as $(B_2 + B_1) > \sqrt{(B_2 - B_1)^2 + 4\sigma\varepsilon}$.

Now we want to prove that all the remaining eigenvalues ($\lambda_5, \lambda_6, \lambda_7$ and λ_8) in Q are negative. To do this we apply the Routh-Hurwitz criteria because the Routh-Hurwitz criterion provides conditions under which all roots of the polynomial Q have negative real parts. The Routh-Hurwitz criterion states that for a polynomial such as Q all roots have negative real parts if and only if all coefficients $Q_i > 0$.

Thus,

$$Q_0 = 1 > 0; Q_1 = (B_3 + B_4 + B_7 + B_8) > 0;$$

$$Q_2 = (B_3B_8 + B_4B_8 + B_3B_7 + B_4B_7 + B_3B_4 - a_1\theta_h + B_7B_8 - a_4\theta_m),$$

$$Q_2 = (B_3B_8 + B_4B_8 + B_3B_7 + B_4B_7 + B_3B_4(1 - R_{0hh}) + B_7B_8(1 - R_{0mm})) > 0 \text{ if } R_{0hh} < 1 \text{ and } R_{0mm} < 1;$$

$$Q_3 = (B_3B_7B_8 - a_4\theta_mB_3 + B_4B_7B_8 - a_4\theta_mB_4 + B_3B_4B_7 - a_1\theta_hB_7 + B_3B_4B_8 - a_1\theta_hB_8),$$

$$Q_3 = (B_3B_7B_8(1 - R_{0mm}) + B_4B_7B_8(1 - R_{0mm}) + B_3B_4B_7(1 - R_{0hh}) + B_3B_4B_8(1 - R_{0hh})) > 0 \text{ if } R_{0hh} < 1 \text{ and } R_{0mm} < 1;$$

$$Q_4 = (B_3B_4B_7B_8 - a_2a_3\theta_h\theta_m - a_1\theta_hB_3B_4 - a_4\theta_mB_7B_8 + a_1a_4\theta_h\theta_m),$$

$$Q_4 = B_3B_4B_7B_8(1 - R_{0mm}R_{0hm} - R_{0hh} - R_{0mm}) + a_1a_4\theta_h\theta_m > 0 \text{ if } R_{0mm}R_{0hm} < 1, R_{0hh} < 1 \text{ and } R_{0mm} < 1.$$

With this analysis the Routh-Hurwitz criterion confirms that the roots of the characteristic polynomial Q also have negative real parts. Thus, all eigenvalues are negative, and the fractional DENV disease free equilibrium point (ξ^f) is locally asymptotically stable when $R_0 < 1$ and unstable when otherwise.

Existence of Backward Bifurcation

In this section, we investigate the possibility of backward bifurcation in the DENV fractional model using the Center Manifold Theorem. Backward bifurcation arises when a stable fractional DENV disease-free equilibrium coexists with a stable fractional DENV endemic equilibrium for the basic reproduction number, $R_0 < 1$. This phenomenon complicates disease control efforts, as reducing R_0 below unity may not eliminate the disease. The Center Manifold Theorem provides a systematic approach to determine the type of bifurcation by analyzing the dynamics near the bifurcation point $R_0 = 1$. Specifically, we calculate the coefficients a and b to classify the bifurcation as forward or backward.

To apply the center manifold theory, the following modification of variables are done on the fractional DENV model (3). We let;

$$H_S = x_1, H_V = x_2, H_E = x_3, H_I = x_4, H_R =$$

$$x_5, M_S = x_6, M_E = x_7 \text{ and } M_I = x_8.$$

Using vector notation

$$X = (x_1, x_2, x_3, x_4, x_5, x_6, x_7, x_8)^T$$

$$\text{Formulated as } \frac{dX}{dt} = F(X)$$

With

$$F = (f_1, f_2, f_3, f_4, f_5, f_6, f_7, f_8)^T$$

Given in the following;

$$\left. \begin{aligned} (a) \quad & {}^c D_t^\alpha x_1 = A_H + \phi_h x_5 + \sigma x_2 - B_1 x_1 \\ (b) \quad & {}^c D_t^\alpha x_2 = \varepsilon x_1 - B_2 x_2 \\ (c) \quad & {}^c D_t^\alpha x_3 = \beta_h x_1 - B_3 x_3 \\ (d) \quad & {}^c D_t^\alpha x_4 = \theta_h x_3 - B_4 x_4 \\ (e) \quad & {}^c D_t^\alpha x_5 = \tau_h x_4 - B_5 x_5 \\ (f) \quad & {}^c D_t^\alpha x_6 = A_M - B_6 x_6 \\ (g) \quad & {}^c D_t^\alpha x_7 = \beta_m x_6 - B_7 x_7 \\ (h) \quad & {}^c D_t^\alpha x_8 = \theta_m x_7 - B_8 x_8 \end{aligned} \right\} \quad (17)$$

And,

$$\beta_h = \frac{\rho_1 x_4 + \rho_2 \omega x_8}{T_{hm}} \text{ and } \beta_m = \frac{\eta_1 \omega x_4 + \eta_2 x_8}{T_{hm}} \quad (18)$$

Suppose, we chose $\rho_2 = \rho_2^*$ as our bifurcation parameter and solve $R_0 = 1$ we have;

$$\rho_2^* = \frac{B_3 B_4 T_{hm} (\mu_h + \varepsilon) (2 - (R_{01} - R_{04}))^2}{4 R_{03} \theta_h \omega A_H (R_{01} - R_{04})^2}$$

Using the fractional DENV Jacobian Matrix evaluated at the fractional DENV disease free equilibrium point J_{ξ^f} with

$$a_2 = \frac{\rho_2^* \omega A_H}{(\mu_h + \varepsilon) T_{hm}}$$

which is in terms of the bifurcation parameter ρ_2^* .

Given that the right eigenvector associated with the simple zero eigenvalue is;

$$W = (w_1, w_2, w_3, w_4, w_5, w_6, w_7, w_8)^T$$

Where $J_{\xi^f} \times W$ can be obtained as;

$$w_4 > 0, w_1 = \frac{B_2 [(a_2 a_3 \theta_m B_5 + a_1 B_5 B_7 B_8 (R_{04} - 1)) + \phi_h \tau_h B_7 B_8 (R_{04} - 1)] w_4}{(\sigma \varepsilon + B_1 B_2) B_5 B_7 B_8 (R_{04} - 1)} > 0 \text{ if } R_{04} > 1,$$

$$w_2 = \frac{\varepsilon w_1}{B_2} > 0, w_3 = \frac{B_4 w_4}{\theta_h} > 0, w_5 = \frac{\tau_h w_4}{B_5} > 0, w_6 =$$

$$\frac{B_7 B_8 a_3 w_4}{B_6 B_7 B_8 (R_{04} - 1)} > 0 \text{ if } R_{04} > 1,$$

$$w_7 = \frac{B_8 a_3 w_4}{B_7 B_8 (R_{04} - 1)} > 0 \text{ if } R_{04} > 1, w_8 = \frac{-a_3 \theta_m w_4}{B_7 B_8 (R_{04} - 1)} <$$

0 if $R_{04} > 1$.

The left eigenvector associated with the simple zero eigenvalue is;

$$V = (v_1, v_2, v_3, v_4, v_5, v_6, v_7, v_8)^T$$

Where $J_{\xi^f}^T \times V$ can be obtained as;

$$\begin{aligned}
 v_1 > 0, v_4 > 0, v_6 = 0, v_3 = \frac{\theta_h v_4}{B_3} > 0, v_5 = \frac{\phi_h v_1}{B_5} > 0, v_8 \\
 &= \frac{B_7(a_1 B_3 v_1 + a_2 \theta_h v_4)}{B_3 B_7 B_8 (R_{04} - 1)} > 0 \text{ if } R_{04} > 1, v_7 \\
 &= \frac{\theta_m v_8}{B_7} > 0 \text{ if } R_{04} > 1.
 \end{aligned}$$

Since $v_6 = 0$ we do not need the derivatives of f_6 . Thus, the derivatives of $f_1, f_2, f_3, f_4, f_5, f_7$ and f_8 that are non zero are;

$$\begin{aligned}
 \frac{\partial^2 f_1}{\partial x_1 \partial x_4} &= \frac{-\rho_1}{T_{hm}}, \frac{\partial^2 f_1}{\partial x_1 \partial x_8} = \frac{-\rho_2^* \omega}{T_{hm}}, \frac{\partial^2 f_3}{\partial x_1 \partial x_4} = \frac{-\rho_1}{T_{hm}}, \frac{\partial^2 f_3}{\partial x_1 \partial x_8} = \\
 \frac{\rho_2^* \omega}{T_{hm}}, \frac{\partial^2 f_7}{\partial x_6 \partial x_4} &= \frac{\eta_1 \omega}{T_{hm}}, \frac{\partial^2 f_7}{\partial x_6 \partial x_8} = \frac{\eta_2}{T_{hm}}.
 \end{aligned}$$

To determine the bifurcation direction at $R_0 = 1$ we consider the signs of a and b which are the bifurcation coefficients as follows;

$$\begin{aligned}
 a &= \sum_{k,i,j=1}^n v_k w_i w_j \frac{\partial^2 f_k(0,0)}{\partial x_i \partial x_j} \\
 a &= v_1 w_1 w_4 \frac{\partial^2 f_1}{\partial x_1 \partial x_4} + v_1 w_1 w_8 \frac{\partial^2 f_1}{\partial x_1 \partial x_8} + v_3 w_1 w_4 \frac{\partial^2 f_3}{\partial x_1 \partial x_4} + \\
 &v_3 w_1 w_8 \frac{\partial^2 f_3}{\partial x_1 \partial x_8} + v_7 w_6 w_4 \frac{\partial^2 f_7}{\partial x_6 \partial x_4} + v_7 w_6 w_8 \frac{\partial^2 f_7}{\partial x_6 \partial x_8}
 \end{aligned}$$

With $v_1 w_1 = 1$ (as $v.w = 1$) we have;

$$a = \left(\frac{\rho_1 w_4 + \rho_2^* \omega w_8}{T_{hm}} \right) (v_3 w_1 - 1) + \left(\frac{\eta_1 \omega w_4 + \eta_2 w_8}{T_{hm}} \right) v_7 w_6$$

Since $w_8 < 0$ at $R_{04} > 1$ then,

$$a < 0$$

if $v_3 w_1 > 1, \rho_2^* \omega w_8 > \rho_1 w_4$ and $\eta_2 w_8 > \eta_1 \omega w_4$.

For when ρ_2^* is the bifurcation parameter

$$\begin{aligned}
 b &= \sum_{k,i,j=1}^n v_k w_i \frac{\partial^2 f_k(0,0)}{\partial x_i \partial \rho_2^*} \\
 b &= v_1 w_1 \frac{\partial^2 f_1}{\partial x_1 \partial \rho_2^*} + v_3 w_1 \frac{\partial^2 f_3}{\partial x_1 \partial \rho_2^*}
 \end{aligned}$$

Where,

$$\frac{\partial^2 f_1}{\partial x_1 \partial \rho_2^*} = \frac{-\rho_2^* \omega x_8}{T_{hm}} \text{ and } \frac{\partial^2 f_3}{\partial x_1 \partial \rho_2^*} = \frac{\rho_2^* \omega x_8}{T_{hm}}$$

So that,

$$b = v_1 w_1 \frac{-\rho_2^* \omega x_8}{T_{hm}} + v_3 w_1 \frac{\rho_2^* \omega x_8}{T_{hm}}$$

With $v_1 w_1 = 1$ (as $v.w = 1$) we have;

$$b = \left(\frac{\rho_2^* \omega x_8}{T_{hm}} \right) (v_3 w_1 - 1)$$

$$b > 0$$

if $v_3 w_1 > 1$.

The analysis of backward bifurcation in the DENV fractional-order model reveals significant insights into the dynamics of the DENV disease. By examining the model through the lens of the center manifold theorem and exploring the conditions for the existence of backward bifurcation and the local stability of the Fractional DENV endemic equilibrium in the

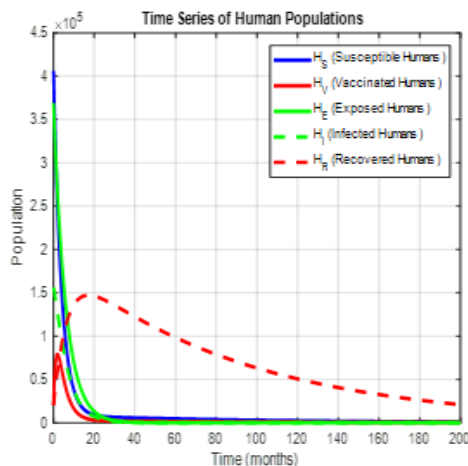
vicinity of the bifurcation point, we found that the disease can persist even when the basic reproduction number, R_0 is less than unity. This phenomenon is critical as it challenges the traditional belief that reducing R_0 below one guarantees the elimination of the DENV disease.

The key finding of this analysis is that backward bifurcation occurs under specific conditions, namely when the parameter a is less than one and b is greater than zero. These conditions imply that, despite R_0 being less than one, multiple equilibrium states exist, including one where the DENV disease remains endemic. This is primarily influenced by the mosquito-to-mosquito transmission dynamics. In particular, when the reproduction number for mosquito-to-mosquito infection, R_{0mm} is greater than one, mosquitoes act as a self-sustaining reservoir for the infection, thereby facilitating the persistence of dengue transmission even when human-related transmission is controlled.

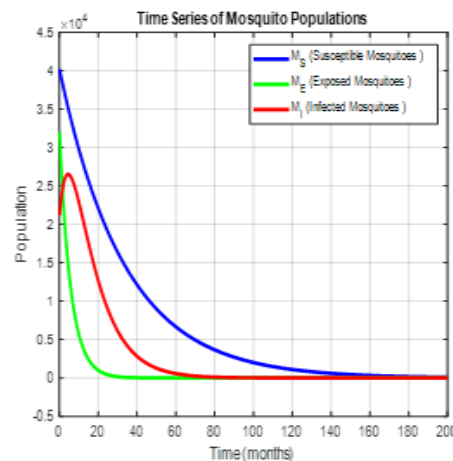
This result underscores the importance of comprehensive intervention strategies. While traditional models suggest that reducing mosquito-to-human transmission is sufficient to control the DENV disease, the existence of backward bifurcation highlights the need for targeted vector control. Measures such as reducing mosquito populations, limiting breeding sites, and deploying insecticide-treated nets become crucial in breaking the cycle of transmission and preventing the persistence of endemic infection, even when R_0 is below one. Thus, the existence of backward bifurcation in this DENV fractional-order model emphasizes the necessity of integrated, sustained interventions targeting both human and mosquito populations. It also stresses the importance of considering the mosquito population as a key factor in DENV disease persistence, offering a more nuanced perspective on the management of dengue epidemics.

RESULTS AND DISCUSSION

In this section, we perform the DENV model numerical analysis presenting the key findings and interpreting their significance within the broader context of the DENV transmission modeling. This section provides both a summary of the outcomes derived from numerical simulations, as well as a discussion of the result outcomes and practical implications for DENV control. The parameter values for the numerical analysis were sourced and recorded in Table 2 with their sources referenced. Using MATLAB Software, the numerical simulation of the DENV model was performed with the initial values in Table 1 and the results obtained are as follows;



(a) Time series simulation of human population

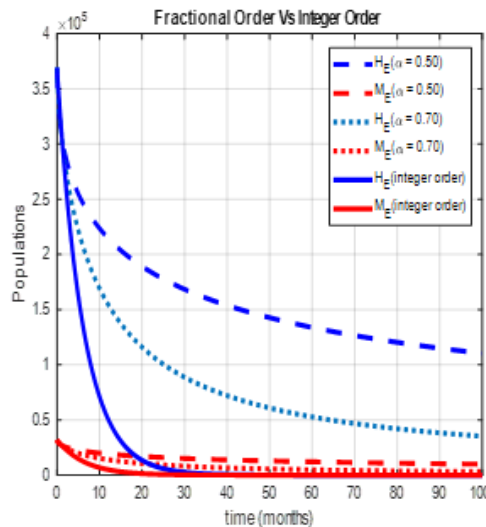


(b) Time series simulation of mosquito population

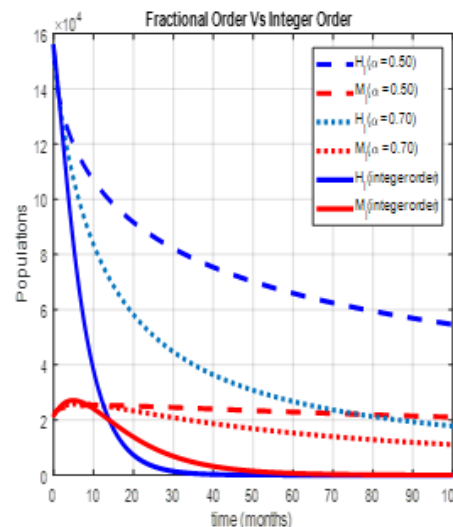
Figure 2: Time series simulation of human and mosquito populations

As shown in Figure 2, panel (a) demonstrates the time-dependent dynamics of human populations during the outbreak. The susceptible population (H_S) rapidly declines within the first few months, while the exposed (H_E) and infected (H_I) populations initially increase and then decrease as recovered individuals (H_R) accumulate. This trend highlights the impact of vaccination and recovery on the

DENV disease mitigation. Panel (b) shows similar dynamics in mosquito populations, where the susceptible and exposed mosquito populations (M_S and M_E) quickly declines, and infected mosquitoes (M_I) peak briefly before subsiding. These results emphasize the importance of intervention strategies targeting both human and mosquito populations.



(a) Simulation of fractional order vs integer order human and mosquito exposed populations

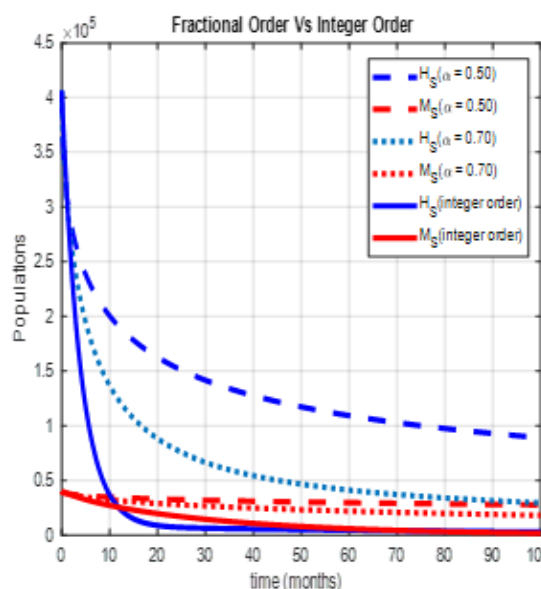


(b) Simulation of fractional order vs integer order human and mosquito infectious populations

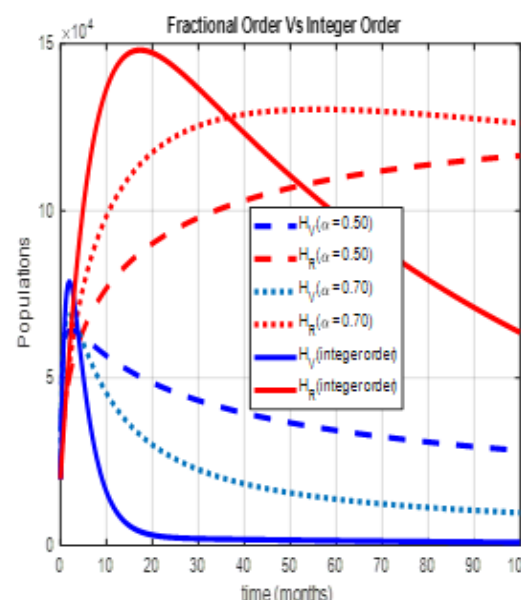
Figure 3: Simulation of fractional order vs integer order human and mosquito exposed with infectious populations

Figure 3 illustrates the effect of fractional-order dynamics on disease progression compared to integer-order models. Panel (a) reveals that for exposed human (H_E) and mosquito (M_E) populations, fractional orders ($\alpha = 0.50, 0.70$) results in slower disease progression, with higher exposed populations persisting over time. Similarly, panel (b) shows that fractional-order dynamics delay the peak and reduce the

magnitude of infectious human (H_I) and mosquito (M_I) populations compared to integer-order models. These findings underscore the flexibility and potential benefits of fractional-order systems in modeling DENV infectious diseases.



(a) Simulation of fractional order vs integer order human mosquito susceptible populations

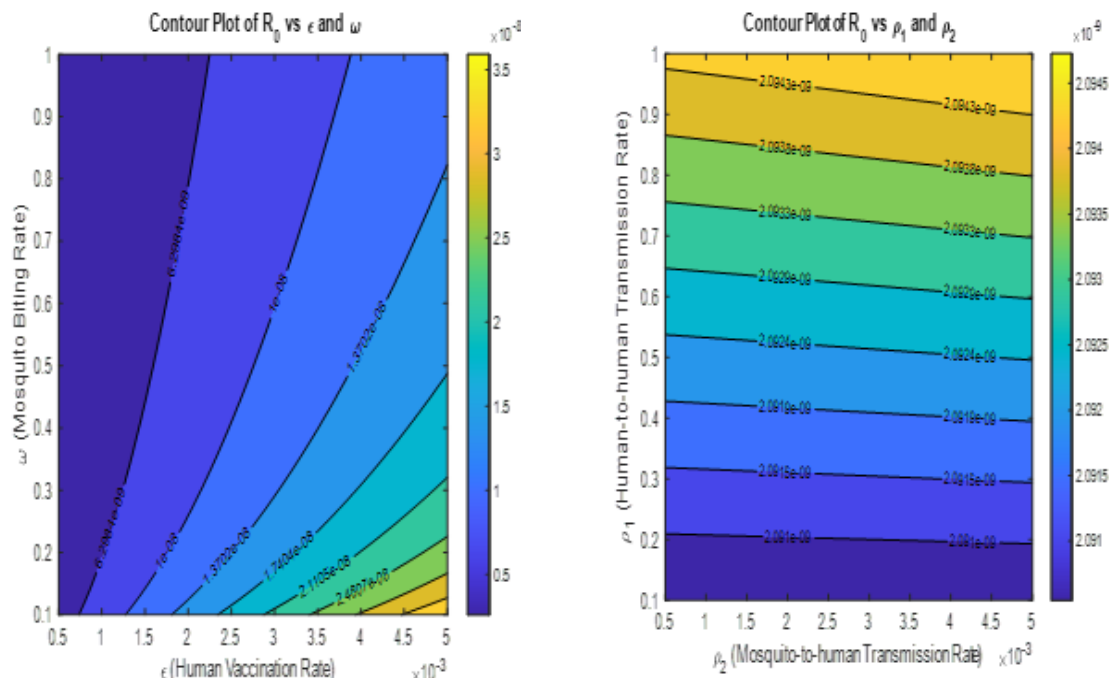


(b) Simulation of fractional order vs integer order human vaccinated and recovered populations

Figure 4: Simulation of fractional order vs integer order human and mosquito susceptible vaccinated with recovered populations

As depicted in Figure 4, fractional-order dynamics affect susceptible, vaccinated, and recovered populations differently. Panel (a) shows that fractional orders ($\alpha = 0.50, 0.70$) slow the decline of susceptible populations (H_S and M_S), reflecting delayed disease spread. Panel (b) reveals that vaccinated humans (H_V) and recovered populations (H_R)

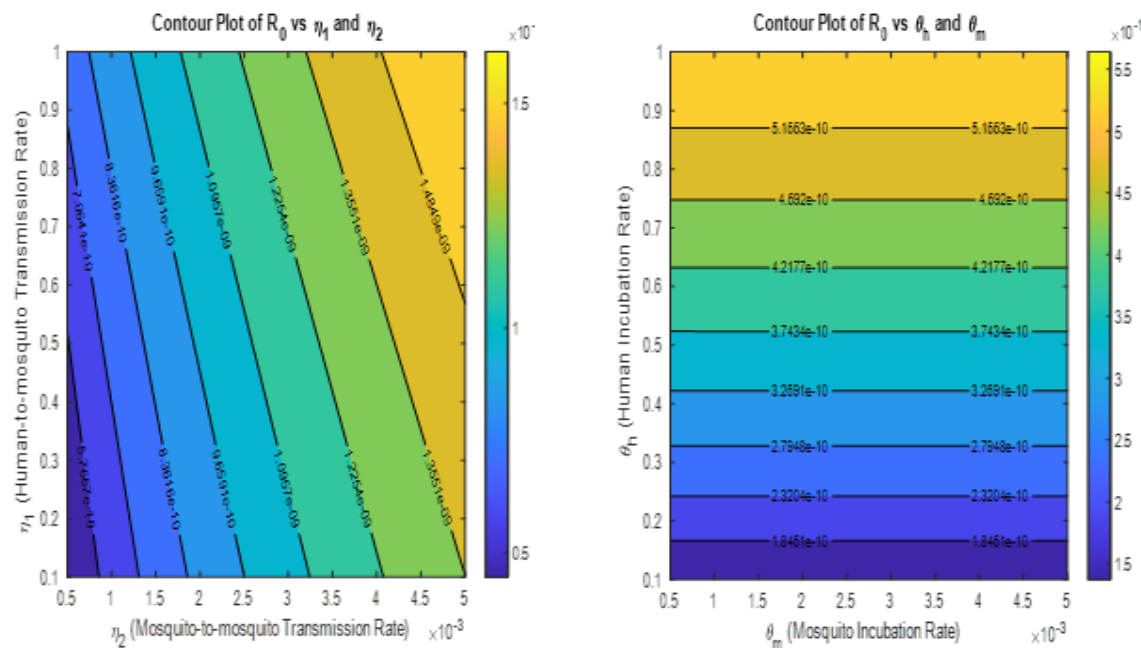
increase more gradually under fractional orders, reaching equilibrium slower than in integer-order cases. These observations highlight the role of fractional-order systems in capturing real-world complexities of population dynamics during DENV epidemics.



(a) Contour plot showing the impact of ω ϵ on R_0 (b) Contour plot showing the impact of ρ_1 and ρ_2 on R_0
 Figure 5: Contour plot showing the impact of ω, ϵ, ρ_1 and ρ_2 on R_0

Figure 5 examines the combined effects of different parameters on R_0 . Panel (a) reveals the interaction between mosquito biting rate (ω) and human vaccination rate (ϵ), demonstrating that increasing vaccination rates can mitigate the effects of higher mosquito activity on R_0 . Panel (b) highlights the influence of transmission rates (ρ_1 and ρ_2),

showing that increasing either parameter significantly amplifies R_0 . These results underscore the critical importance of reducing transmission and enhancing vaccination efforts to control outbreaks.



(a) Contour plot showing the impact η_1 and η_2 , on R_0 (b) Contour plot showing the impact θ_h and θ_m on R_0
 Figure 6: Contour plot showing the impact η_1, η_2, θ_h and θ_m on R_0

The contour plots in Figure 6 highlight the role of transmission and incubation rates in influencing R_0 , which is a critical measure of disease spread. Panel (a) focuses on transmission rates (η_1 and η_2). It demonstrates that higher values of both transmission parameters increase R_0 . This indicates that effective transmission between humans and mosquitoes (and mosquitoes and mosquitoes) enhances the epidemic potential. To mitigate R_0 , we might include reducing contact rates between mosquitoes and humans, such as implementing vector control measures or encouraging the

use of protective measures like insecticide-treated bed nets. Panel (b) shows how the human (θ_h) and mosquito (θ_m) incubation rates affect R_0 . Higher incubation rates result in larger R_0 , indicating that quicker development of infectiousness in both humans and mosquitoes accelerates the transmission cycle. Targeting incubation rates through interventions such as antivirals could help slow the development of infectious stages and reduce R_0 .

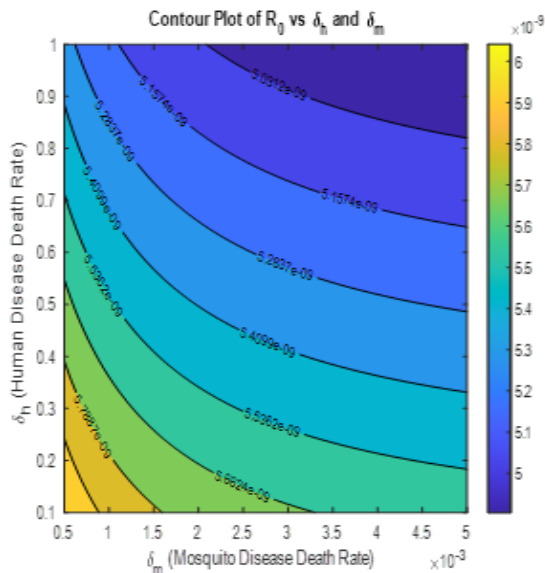


Figure 7: Contour plot showing the impact of δ_h and δ_m on R_0
 Figure 7: Contour plot showing the impact of $\delta_h, \delta_m, \Lambda_H$ and Λ_M on R_0

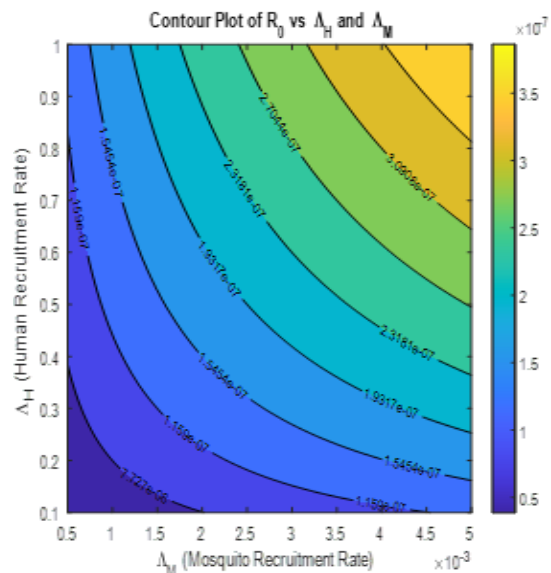


Figure 7: Contour plot showing the impact of Λ_H and Λ_M on R_0

The contour plots in Figure 7 explore the effects of mortality and recruitment rates of the human and mosquito populations on R_0 . Panel (a) illustrates the effect of disease-induced death rates (δ_h and δ_m) in humans and mosquitoes. Higher death rates reduce R_0 , as mortality limits the number of individuals contributing to the transmission cycle. While disease-induced mortality naturally curtails transmission, interventions that reduce infection rates (e.g., vaccines or vector reduction) are more desirable as they minimize mortality without relying on

population depletion. Panel (b) focuses on the recruitment rates (Λ_H and Λ_M) of humans and mosquitoes. Higher recruitment rates result in a larger R_0 , as more individuals in the population sustain the transmission cycle. Strategies to limit recruitment (e.g., reducing vector breeding sites for mosquitoes) could significantly reduce R_0 and help control disease spread.

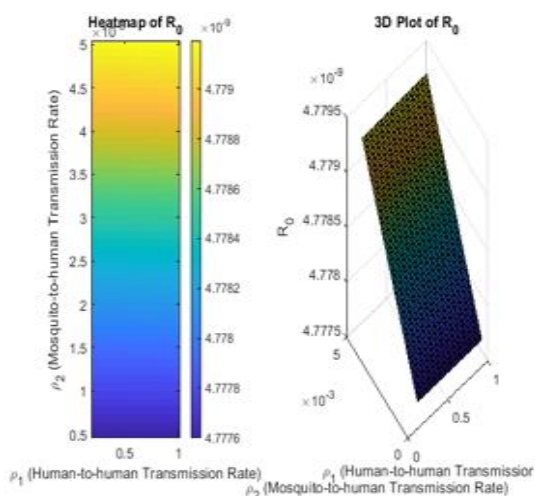


Figure 8: Heatmap vs 3D plot showing the impact of ρ_1 and ρ_2 on R_0
 Figure 8: Heatmap vs 3D plot showing the impact of ρ_1, ρ_2, θ_h and θ_m on R_0

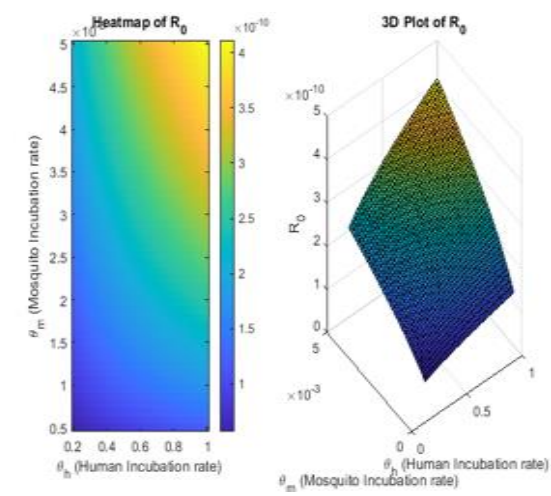


Figure 8: Heatmap vs 3D plot showing the impact of θ_h and θ_m on R_0

Figure 8 highlights the influence of transmission and incubation rates on R_0 . In panel (a), R_0 increases sharply with higher human-to-human (ρ_1) and mosquito-to-human (ρ_2) transmission rates, indicating their pivotal role in DENV disease spread. Panel (b) illustrates how increasing human (θ_h)

and mosquito (θ_m) incubation rates further amplify R_0 . These findings emphasize the need for interventions targeting transmission and incubation stages of the disease.

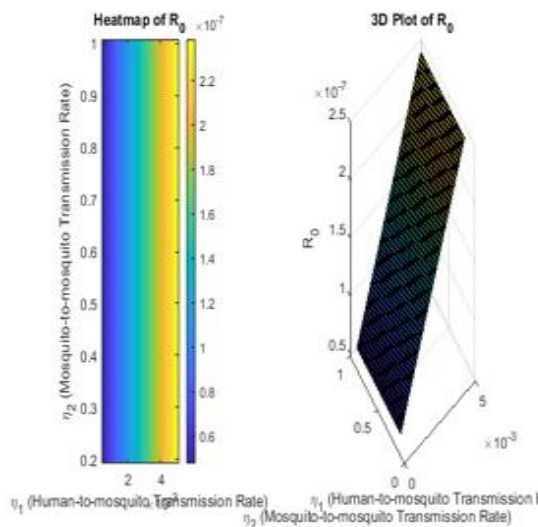


Figure 9: Heatmap vs 3D plot showing the impact of η_1 and η_2 on R_0

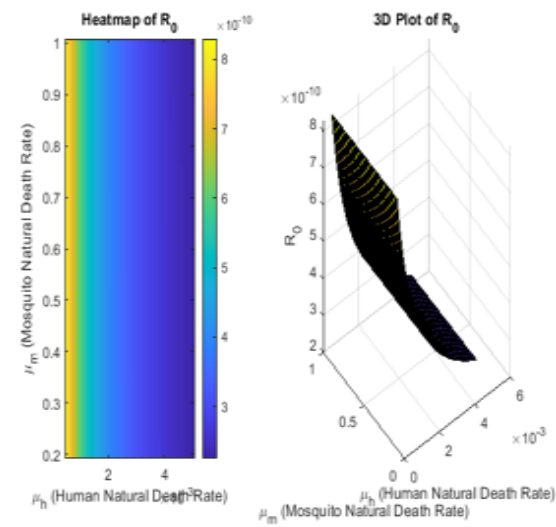


Figure 9: Heatmap vs 3D plot showing the impact of μ_h and μ_m on R_0

Figure 9: Heatmap vs 3D plot showing the impact of η_1, η_2, μ_h

and μ_m on R_0 . Figure 9 demonstrates the impact of mosquito-to-human (η_1) and human-to-mosquito (η_2) transmission rates, as well as natural death rates, on R_0 . Panel (a) shows that higher transmission rates (η_1 and η_2) dramatically increase R_0 , while panel (b) reveals that increasing natural death rates (μ_h and μ_m) reduces R_0 . The findings highlight the importance of strategies that disrupt transmission cycles and increase vector mortality to lower R_0 .

Discussion

The results of this study underscore the utility of fractional-order modeling in capturing the nuanced dynamics of DENV transmission. By incorporating memory effects through the Caputo fractional derivative, the model demonstrated improved realism in representing both transient and long-term epidemic behaviors. The findings revealed several key insights into the dynamics of DENV transmission, the implications of which resonate with existing literature and public health strategies.

One of the most striking aspects of the DENV model was its ability to delay the peak of infectious populations. This aligns with findings from previous studies, such as Alshehry et al. (2024), which observed that fractional models offer a more accurate representation of transient dynamics compared to integer-order models. Particularly in early outbreak phases, our results corroborate these observations, showing the persistence of higher exposed populations. This delayed peak is a critical feature for designing effective intervention strategies, as it indicates that fractional models better reflect the gradual buildup of infectious cases, providing a more accurate prediction of the DENV disease's progression.

In addition to the delayed epidemic peaks, the sensitivity of the basic reproduction number to key transmission parameters such as human-to-human and mosquito-to-human interactions is a noteworthy finding. This mirrors conclusions drawn by Pandey & Phaijoo (2024), who emphasized the critical role of intervention strategies targeting these parameters, such as vaccination campaigns and vector control measures. Our

results further validate the efficacy of these strategies, demonstrating significant reductions in the basic reproduction number when transmission rates are curtailed through control efforts. This reinforces the importance of tailoring public health interventions to specifically address high-transmission pathways.

However, the fractional-order model introduces an additional complexity which is the influence of memory effects on DENV dynamics, which is not accounted for in traditional integer-order models. This is consistent with previous observations by Usman et al. (2024), and Meena & Purohit (2024), who emphasized the importance of early interventions, such as accelerating recovery rates or deploying antivirals, to prevent prolonged outbreaks. Our contour plot analysis reinforced these conclusions, illustrating how adjustments to incubation-related parameters can dampen epidemic severity. More importantly, the model's ability to simulate memory effects stresses the need for sustained interventions, as these effects can amplify delays in epidemic peaks and prolong outbreak durations.

An essential feature of the DENV model's dynamics is the interplay between human and mosquito populations, particularly the mosquito-to-mosquito transmission route. The concept of backward bifurcation, highlighted by the existence of multiple stable equilibria, has profound implications for the management of DENV epidemics. When the mosquito-to-mosquito reproduction number, $R_{0_{mm}}$ is greater than one, even when R_0 less than one, the DENV disease is can persist in the population. This situation is particularly relevant in areas with high mosquito densities, where mosquitoes act as a self-sustaining reservoir for the infection. Despite efforts to control human-to-human transmission through vaccination, the presence of mosquito-to-mosquito transmission could maintain endemicity, especially if mosquito control measures are insufficient. This dynamic reinforces the necessity of integrated control strategies that address both human and mosquito populations concurrently.

The persistence of exposed populations in fractional-order dynamics, influenced by the fractional DENV model's memory effects, underlines the importance of coordinated, long-term intervention efforts. Our results suggest that while vaccination campaigns are critical, they should be complemented by robust mosquito control measures, such as the removal of breeding sites and the use of insecticide-treated nets. Furthermore, the optimal timing of interventions becomes increasingly important in light of the delayed peaks, emphasizing the need for public health authorities to act preemptively before critical infection thresholds are reached.

The existence of backward bifurcation calls for a shift in how we approach DENV control. While traditional models predict that reducing R_0 below unity ensures the elimination of the DENV disease, the phenomenon of backward bifurcation challenges this assumption. Instead, the mosquito population must be carefully managed to prevent the re-establishment of endemic transmission. Integrated strategies, such as combining vaccination with vector control and public health education, are crucial in breaking the cycle of dengue transmission and preventing further outbreaks.

Despite the valuable insights offered by this model, several limitations should be acknowledged. The assumption of homogeneous mixing of human and mosquito populations may not accurately reflect the spatial heterogeneities and localized transmission dynamics that are often observed in dengue outbreaks. Future models could incorporate spatial components, allowing for a more detailed understanding of how localized interventions might be more effective in certain areas. Additionally, the model's reliance on parameters derived from general literature does not account for region-specific factors such as climate, healthcare infrastructure, and population density. Integrating more localized data could enhance the accuracy and applicability of the model, particularly in predicting seasonal outbreaks that are influenced by factors like temperature and rainfall.

Furthermore, the model does not consider age-structured populations or immunity variations within the human population, which are important for understanding the differential impact of vaccination strategies across age groups. Age-specific immunity and vaccination efficacy could significantly influence the outcomes of vaccination campaigns, particularly in areas where immunity levels vary. Finally, while the Caputo fractional derivative enables the modeling of memory effects, the computational complexity of fractional-order models can limit their scalability for larger systems or real-time application in public health decision-making. Advances in numerical methods and computational techniques, such as adaptive step-size strategies or parallelized algorithms, will be essential for improving the practical utility of these models in dynamic epidemiological settings.

Looking ahead, there are many opportunities for further research. Integrating region-specific data, exploring advanced intervention strategies, and considering the dynamic behaviors of mosquitoes in different environmental contexts could improve the model's accuracy and predictive power. Moreover, the integration of real-world data into the fractional-order framework will be essential for model validation and improving its capacity to inform public health policies and strategies. Ultimately, fractional-order models can provide a powerful tool for understanding and controlling the complexities of dengue transmission, especially when combined with targeted interventions informed by the detailed dynamics revealed through backward bifurcation analysis.

In conclusion, the findings of this study highlight the critical importance of considering both mosquito and human populations in dengue control. The incorporation of memory effects and the exploration of backward bifurcation underscore the need for integrated, long-term strategies in the fight against dengue. By leveraging these advanced modeling techniques, public health interventions can be more strategically timed and better tailored to the local dynamics of dengue transmission, ultimately helping to reduce the burden of this global disease.

CONCLUSION

This study presents a novel fractional-order mathematical model for dengue virus (DENV) transmission that incorporates memory effects and both vector and non-vector transmission pathways. By leveraging the Caputo fractional derivative, the model provides a more realistic framework for analyzing dengue dynamics, capturing both short-term and long-term epidemic behaviors. The inclusion of vaccination dynamics and human movement strengthens its applicability to real-world scenarios, reflecting the complex interplay between disease spread and intervention strategies. Key findings reveal that fractional-order modeling effectively delays epidemic peaks and extends the duration of exposure among populations, providing a more gradual buildup of infectious cases over time. This delayed progression is crucial for planning timely and targeted interventions. Sensitivity analysis of the basic reproduction number underscores the importance of interventions focused on reducing mosquito-to-human transmission, particularly through vaccination campaigns and vector control measures. These results are consistent with existing literature, reinforcing the critical role of integrated strategies, combining vaccination, vector control, and public awareness, in managing dengue outbreaks. The practical implications for public health decision-making are significant. Fractional-order models enable more precise predictions of epidemic dynamics, allowing for optimized intervention timing and resource allocation. Targeting high-transmission pathways at the right moment can effectively reduce disease spread before infection levels reach critical thresholds. These insights highlight the necessity of sustained and coordinated interventions to manage long-term dengue dynamics, particularly in regions prone to recurrent outbreaks. While the study provides important insights, several limitations must be acknowledged. The model assumes homogeneous mixing, which may not capture spatial heterogeneities in transmission dynamics. Additionally, generalized parameter values limit the model's applicability to specific regions. Future work should focus on incorporating region-specific data, spatial heterogeneity, and age-structured populations to enhance model accuracy and relevance. Further advancements in computational methods are also necessary to address the challenges of solving fractional-order equations, particularly for large-scale systems and real-time applications. In conclusion, this study highlights the transformative potential of fractional-order modeling in understanding and controlling dengue epidemics. By capturing memory effects and incorporating both vector and non-vector pathways, the model provides a comprehensive approach to DENV disease dynamics. The findings underscore the value of these models in informing evidence-based public health strategies, particularly in regions with high dengue prevalence. Moving forward, refining these models through local data integration and improved computational techniques will enhance their utility in managing and mitigating dengue outbreaks across diverse contexts.

List of abbreviations

WHO - World Health Organization .
DFE - Disease Free Equilibrium.
EE - Endemic Equilibrium.
LAS - Locally Asymptotically Stable.

REFERENCES

- Adel, W., Elsonbaty, A., & Mahdy, A. M. S. (2024). On some recent advances in fractional order modeling in engineering and science. *Computation and Modeling for Fractional Order Systems*, 169–197.
- Alshehry, A. S., Yasmin, H., Khammash, A. A., & Shah, R. (2024). Numerical analysis of dengue transmission model using Caputo–Fabrizio fractional derivative. *Open Physics*, 22(1), 20230169.
- Asaduzzaman, M., Kilicman, A., Al-Mamun, A., & Hossain, M. D. (2024). Analysis of a novel conformable fractional order ASIR dengue transmission model in the perspective of Bangladesh. *Mathematical Models and Computer Simulations*, 16(3), 431–456.
- Atokolo, W., Aja, R. O., Omale, D., Ahman, Q. O., Acheneje, G. O., & Amos, J. (2024). Fractional mathematical model for the transmission dynamics and control of Lassa fever. *Franklin Open*, 7(15), 2773–1863.
- Chitnis, N., Smith, T., & Schapira, A. (2021). The role of vertical transmission in the spread of mosquito-borne diseases: Insights from a dengue model. *Journal of Theoretical Biology*, 523, 110713. <https://doi.org/10.1016/j.jtbi.2021.110713>.
- El-Shenawy, A., El-Gamel, M., & Teba, A. (2024). Simulation of the SIR dengue fever nonlinear model: A numerical approach. *Partial Differential Equations in Applied Mathematics*, 11, 100891.
- Islam, N., Borhan, J. R. M., & Prodhan, R. (2024). Application of mathematical modeling: A mathematical model for dengue disease in Bangladesh. *International Journal of Mathematical Sciences and Computing*, 10(1), 19–30.
- Kumar, R., Saxena, B., Shrivastava, R., & Bhardwaj, R. (2024). Mathematical modeling of dengue disease transmission dynamics. *Indian Journal of Science and Technology*, 17(39), 4101–4110.
- Meena, M., & Purohit, M. (2024). Mathematical analysis using fractional operator to study the dynamics of dengue fever. *Physica Scripta*, 99(9), 095206.
- Meetei, M. Z., Zafar, S., Zaagan, A. A., Mahnashi, A. M., & Idrees, M. (2024). Dengue transmission dynamics: A fractional-order approach with compartmental modeling. *Fractal and Fractional*, 8(4), 207.
- Mohammed, A., Abdulfatai, A., Abimbola, N. G. A., & Ali, I. M. (2022). Mathematical modelling of dengue fever incorporating vaccination as control. *Abacus (Mathematics Science Series)*, 49(1).
- Naaly, B. Z., Marijani, T., Isdory, A., & Ndendya, J. Z. (2024). Mathematical modeling of the effects of vector control, treatment and mass awareness on the transmission dynamics of dengue fever. *Computer Methods and Programs in Biomedicine Update*, 6, 100159.
- Nisar, K. S., Farman, M., Abdel-Aty, M., & Ravichandran, C. (2024). A review of fractional order epidemic models for life sciences problems: Past, present and future. *Alexandria Engineering Journal*, 95, 283–305.
- Olayiwola, M. O., & Alaje, A. I. (2024). Mathematical analysis of intrahost spread and control of dengue virus: Unraveling the crucial role of antigenic immunity. *Franklin Open*, 100117.
- Olayiwola, M. O., & Yunus, A. O. (2024). Mathematical analysis of a within-host dengue virus dynamics model with adaptive immunity using Caputo fractional-order derivatives. *Journal of Umm Al-Qura University for Applied Sciences*, 1–20.
- Pandey, H. R., & Phaijoo, G. R. (2024). Dengue dynamics in Nepal: A Caputo fractional model with optimal control strategies. *Heliyon*, 10(13).
- Rahman, A., Khan, M., & Islam, S. (2022). Modeling rare human-to-human transmission routes in dengue dynamics. *Journal of Infectious Diseases and Epidemiology*, 10(3), 56–65. <https://doi.org/10.1016/j.jide.2022.05.003>.
- Shanmugam, S. N., & Byeon, H. (2024). Comprehending symmetry in epidemiology: A review of analytical methods and insights from models of COVID-19, Ebola, dengue, and monkeypox. *Medicine*, 103(41), e40063.
- Sk, T., Bal, K., Biswas, S., & Sardar, T. (2024). Global stability and optimal control in a single-strain dengue model with fractional-order transmission and recovery process. *arXiv preprint*, arXiv:2402.11974.
- Usman, M., Abbas, M., Khan, S. H., & Omame, A. (2024). Analysis of a fractional-order model for dengue transmission dynamics with quarantine and vaccination measures. *Scientific Reports*, 14(1), 11954.
- Vellappandi, M., Govindaraj, V., Kumar, P., & Nisar, K. S. (2024). An optimal control problem for dengue fever model using Caputo fractional derivatives. *Progress in Fractional Differentiation*, 10(1), 1–15.
- Vijayalakshmi, G. M., Ariyanatchi, M., Cepova, L., & Karthik, K. (2024). Advanced optimal control approaches for immune boosting and clinical treatment to enhance dengue viremia models using ABC fractional-order analysis. *Frontiers in Public Health*, 12, 1398325.
- World Health Organization (WHO). (2022). Dengue and severe dengue. *WHO Fact Sheets*. Retrieved from <https://www.who.int/newsroom/fact-sheets/detail/dengue-and-severe-dengue>.
- Xu, Z., Zhang, H., Yang, D., Wei, D., Demongeot, J., & Zeng, Q. (2024). The mathematical modeling of the host–virus interaction in dengue virus infection: A quantitative study. *Viruses*, 16(2), 216.

